COMMUNICATIONS CHEMISTRY

ARTICLE

https://doi.org/10.1038/s42004-019-0215-3 OPEN

Unique acrylic resins with aromatic side chains by homopolymerization of cinnamic monomers

Motosuke Imada [1,2,3], Yasumasa Takenaka [1], Hidehito Hatanaka[1,2], Takeharu Tsuge[2] & Hideki Abe[1,2]

Cinnamic monomers, which are useful chemicals derived from biomass, contain α,β-unsaturated carbonyl groups with an aromatic ring at the β-position. Homopolymers synthesized by addition polymerization of these compounds are expected to be innovative bio-based polymer materials, as they have both polystyrene and polyacrylate structures. However, polymerization of these compounds by many methods is challenging, including by radical methods, owing to steric hindrance of the substituents and delocalization of electrons throughout the molecule via unsaturated π-bonding. Herein we report that homopolymers of these compounds with molecular weights (M_n) of ~18,100 g mol^{-1} and controlled polymer backbones can be synthesized by the group-transfer polymerization technique using organic acid catalysts. Additionally, these homopolymers are shown to have high heat resistance comparable to that of engineering plastics. Overall, these findings may open up possibilities for the convenient homopolymerization of cinnamic monomers to produce high-performance polymer materials.

[1] Bioplastic Research Team, RIKEN Center for Sustainable Resource Science, 2-1 Hirosawa, Wako, Saitama 351-0198, Japan. [2] Department of Material Science and Engineering, Tokyo Institute of Technology, 4259 Nagatsuta, Midori-ku, Yokohama 226-8502, Japan. [3] Research Center, Innovation and Business Development Division, Nippon Shokubai Co., Ltd., 5-8 Nishi Otabi-cho, Suita, Osaka 564-0034, Japan. Correspondence and requests for materials should be addressed to Y.T. (email: yasumasa.takenaka@riken.jp)

Bio-based plastics can be sustainably produced from biomass, a renewable resource, without using fossil fuels. As such, these environmentally friendly polymer materials are carbon neutral and their production will lead to a reduction in CO_2 emissions. Therefore, the development of high-performance bio-based plastics derived from renewable resources has received considerable interest in recent years[1–6]. For example, the high-performance bio-based polyimides recently developed by Suvannasara et al. using 4-aminocinnamic acid derived from genetically manipulated *Escherichia coli* show ultrahigh thermal resistance with T_{d10} values higher than 425 °C[6].

Cinnamic monomers are aromatic compounds that can be extracted from certain plants, such as *Cinnamomum cassia*, and derived by thermal decomposition of lignin, a complex phenolic biopolymer comprising wood or straw fiber cell walls along with cellulose[7–9]. Characteristically, these compounds have an aromatic substituent at the β-position of an α,β-unsaturated carbonyl group. Notably, successful polymerization of these compounds at only the carbon–carbon double bond moiety would produce polymers with a linear saturated carbon–carbon skeleton as the polymer backbone and alternating aromatic rings and carboxylate (or ester) groups as side chains. Owing to this structure, such polymers are expected to be applicable as high-performance and multifunctional bio-based polymeric materials that combine the features of both polystyrene (PSt) and acrylic resins. Further, they may possess high heat resistance and a rigid polymer backbone derived from the interactions between aromatic side chains and the ditacticity attributed to α- and β- substituents.

However, convenient addition polymerization of cinnamic monomers has rarely been reported owing to steric hindrance of the aromatic substituent located at the β-position and delocalization of the electrons throughout the molecule via unsaturated π-bonding[10–18]. Sapiro et al. reported the polymerization of ethyl cinnamate under harsh high-temperature and high-pressure conditions (125 °C, 4,000 atm)[10]. A white powdery product was obtained in moderate yield (58.5%), but the molecular weight of the product was not provided. Marvel et al. reported that the radical polymerization of cinnamates using 2,2′-azobisisobutyronitrile (AIBN) as an initiator for a long period of 1 month gave a white powdery product in low yield (10%)[11]. In addition to the inefficiency of these methods, polymerization at only the carbon–carbon double bonds was not clearly demonstrated. Moreover, a comprehensive evaluation of the physical properties of these polymers is required.

As an alternative to these methods, Terao et al. reported the copolymerization of cinnamic monomers with vinyl monomers, such as methyl acrylate or styrene, via living radical methods including metal-catalyzed living radical polymerization, atom transfer radical polymerization, reversible addition-fragmentation chain transfer polymerization, and nitroxide-mediated polymerization[19]. However, as the incorporation of cinnamic monomers into the copolymers ranged from 15 to 40 mol%, the obtained materials are unlikely to exhibit the properties expected for homopolymers of cinnamic compounds. Therefore, the development of a convenient homopolymerization system for cinnamic monomers is highly desirable.

Alkyl crotonates are α,β-unsaturated carbonyl compounds with a methyl group at the β-position. Similar to cinnamic monomers, there are well-known difficulties in using alkyl crotonates (or crotonic acid) as a monomer to produce polymers with sufficient molecular weights by classical radical polymerization methods using AIBN or benzoyl peroxide and by typical anionic polymerization methods using an alkyl lithium or Grignard reagent[17–22]. Group-transfer polymerization (GTP) systems for various alkyl crotonates have been developed using a Lewis acid (HgI_2 or CdI_2) as a catalyst and iodotrialkylsilane as a cocatalyst[23–27]. Chen and co-workers reported an efficient catalytic Lewis pair polymerization system for methyl crotonate using *N*-heterocyclic carbene as a Lewis base and an aluminum or a boron compound as a Lewis acid[28,29]. Additionally, organic-acid-catalyzed GTP systems were developed by Chen and co-workers and Kakuchi et al. for the polymerization of (meth)acrylates[30–32]. In the last year, we applied such an organic-acid-catalyzed GTP system to the polymerization of various alkyl crotonates[33,34]. The GTP system in our study used an organic acid such as *N*-(trimethylsilyl)bis(trifluoromethanesulfonyl)imide (Tf_2NTMS) as a catalyst and a silyl ketene acetal such as 1-methoxy-1-(trimethylsiloxy)-2-methyl-1-propene (MTS) as an initiator (Supplementary Fig. 1). Owing to the success of this approach for polymerizing alkyl crotonates, it is possible that it could be modified to realize the convenient homopolymerization of cinnamic monomers.

Herein, we successfully apply an organic-acid-catalyzed GTP system to the polymerization of alkyl cinnamates and their derivatives to produce homopolymers with molecular weights (M_n) of ~18,100 g mol^{-1}. Structural characterization of the obtained polymers using NMR spectroscopy and matrix-assisted laser desorption/ionization time-of-flight mass spectrometry (MALDI-TOF-MS), as well as determination of the molecular structures of their low-molecular-weight homologs by single-crystal X-ray structural analysis, confirms that polymerization proceeds at only the carbon–carbon double bond moiety. In addition, evaluation of the thermal properties (thermal decomposition temperature (T_d) and glass transition temperature (T_g)) of the obtained polymers using thermogravimetric analysis (TGA) and dynamic mechanical analysis (DMA) reveals these materials to have high thermal stabilities.

Results

Polymerization of cinnamates and their derivatives by GTP. The polymerization of alkyl cinnamates and their derivatives was performed by the GTP technique in the presence of MTS as an initiator and various organic acid catalysts. Table 1 summarizes the yields and molecular weights of the obtained polymers. When GTP was performed for 7 days with methyl cinnamate as a monomer in the presence of Tf_2NTMS at temperatures ranging from room temperature to −35 °C, corresponding poly(methyl cinnamate)s were obtained with number-average molecular weights (M_n) ranging from 7,300 to 13,000 g mol^{-1}, yields ranging from 23 to 46%, and dispersities ($Đ$s) ranging from 1.47 to 1.84 (Entries 1–4, Table 1). Notably, poly(methyl cinnamate) with a relatively high number-average molecular weight (M_n = 13,000 g mol^{-1}) and a narrow $Đ$ (1.47) was obtained when polymerization was allowed to proceed for 7 days at −35 °C (Entry 4, Table 1), whereas a M_n of only 7,300 g mol^{-1} was achieved for the reaction carried out at room temperature (Entry 1, Table 1). This result suggests that side reactions including intramolecular termination reactions, such as cyclization and/or isomerization of the propagating chain-end groups, as proposed for the GTP of methacrylate, were suppressed at low temperatures (−35 °C), with the propagation reaction proceeding preferentially[35–37] (Supplementary Fig. 2). However, when the polymerization was performed at lower temperatures such as −80 °C, the unreacted monomers and the reaction products precipitated in the reaction solution owing to their low solubilities.

Next, we investigated various conditions for GTP at −35 °C. When the feed ratio of monomer to initiator was varied from 50 to 25 (mol mol^{-1}) for GTP performed for 14 days at −35 °C, the value of the molecular weight divided by the yield of the obtained polymer was proportional to this feed ratio (Entries 5–9, Table 1) (Supplementary Fig. 3). This result indicates

Table 1 GTP of cinnamates and their derivatives with MTS in the presence of various organic acid catalysts[a]

Entry	Monomer	Initiator (mmol)	Catalyst (mmol)		CH_2Cl_2 (mL)	Temp (°C)	Time (day)	Polymer yield (%)	M_n[b] (g mol^{-1})	$Đ$[b] (M_w/M_n)
1	Methyl cinnamate	0.26	Tf_2NTMS	0.26	7.5	rt	7	23	7,300	1.60
2	Methyl cinnamate	0.26	Tf_2NTMS	0.26	7.5	0	7	34	12,000	1.81
3	Methyl cinnamate	0.26	Tf_2NTMS	0.26	7.5	−20	7	46	12,200	1.84
4	Methyl cinnamate	0.26	Tf_2NTMS	0.26	7.5	−35	7	43	13,000	1.47
5	Methyl cinnamate	0.26	Tf_2NTMS	0.26	7.5	−35	14	69	15,000	1.69
6	Methyl cinnamate	0.33	Tf_2NTMS	0.26	7.5	−35	14	84	14,400	1.37
7	Methyl cinnamate	0.37	Tf_2NTMS	0.26	7.5	−35	14	89	12,200	1.41
8	Methyl cinnamate	0.43	Tf_2NTMS	0.26	7.5	−35	14	88	9,500	1.48
9	Methyl cinnamate	0.52	Tf_2NTMS	0.26	7.5	−35	14	85	7,500	1.49
10	Methyl cinnamate	0.26	Tf_2NTMS	0.26	7.5	−35	28	81	18,100	1.90
11	Methyl cinnamate	0.26	Tf_2NTMS	1.30	7.5	−35	7	75	17,800	1.73
12	Methyl cinnamate	0.26	Tf_2NTMS	0.05	12.5	−35	7	22	4,200	1.27
13	Methyl cinnamate	0.26	$C_6F_5CHTf_2$	0.05	12.5	−35	7	9	4,600	1.30
14	Methyl cinnamate	0.26	Tf_2NH	0.05	12.5	−35	7	14	4,500	1.27
15	Methyl cinnamate	0.26	$Ph_3C[B(C_6F_5)_4]$	0.05	12.5	−35	7	8	4,200	1.28
16	Methyl cinnamate	0.26	Tf_2NTMS	0.26	12.5	−35	7	35	7,300	1.27
17	Ethyl cinnamate	0.26	Tf_2NTMS	0.26	12.5	−35	7	6	3,800	1.10
18	Isopropyl cinnamate	0.26	Tf_2NTMS	0.26	12.5	−35	7	trace	800	1.06
19	Methyl 4-methyl cinnamate	0.26	Tf_2NTMS	0.26	12.5	−35	7	35	8,300	1.16
20	Methyl 4-methoxy cinnamate	0.26	Tf_2NTMS	0.26	12.5	−35	7	66	3,000	1.48
21	Methyl 3,4-dimethoxy cinnamate	0.26	Tf_2NTMS	0.26	12.5	−35	7	none[c]	–	–
22	Methyl 3,4,5-trimethoxy cinnamate	0.26	Tf_2NTMS	0.26	12.5	−35	7	none[c]	–	–

[a]Monomer, 13 mmol. All experiments were performed in a dry argon atmosphere
[b]Number-average molecular weight (M_n) and dispersity ($Đ$) were determined using conventional GPC against PSt standards in $CHCl_3$
[c]Polymer was not obtained

that this polymerization proceeds through the general GTP mechanism. Using the reaction conditions of Entry 4 but extending the reaction time to 28 days increased the yield and M_n of the obtained polymer from 43 to 81% and from 13,000 to 18,100 g mol^{-1}, respectively (Entry 10, Table 1). This result is a remarkable example of the convenient homopolymerization of cinnamates under mild conditions as compared to the literature data[10–18].

Furthermore, we investigated the effect of the catalyst in the GTP system. Various organic acid catalysts, including 1-[bis (trifluoromethanesulfonyl)methyl]-2,3,4,5,6-pentafluorobenzene ($C_6F_5CHTf_2$), bis(trifluoromethanesulfonyl)imide (Tf_2NH), and triphenylmethylium tetrakis(pentafluorophenyl)borate ($Ph_3C[B(C_6F_5)_4]$), all gave the corresponding methyl cinnamate polymer. However, these catalysts were less active than Tf_2NTMS for the GTP of methyl cinnamate (Entries 12–15, Table 1). The convenient polymerization of methyl cinnamate prompted us to investigate the polymerization activities of various monomers in the GTP system using Tf_2NTMS.

Therefore, we examined the GTP of various monomers using Tf_2NTMS (Entries 16–22, Table 1). The effect of an ester substituent was studied by comparing the polymerizations of ethyl cinnamate and *iso*-propyl cinnamate. As expected, the polymer yield decreased when the bulkiness of the ester substituent of the alkyl cinnamates increased (*iso*-propyl > ethyl > methyl) because the steric hindrance of the ester substituent inhibited polymerization. Unexpectedly, as the bulkiness of the ester substituent of the alkyl cinnamates increased, the $Đ$ of the obtained polymer narrowed from 1.27 (methyl cinnamate) to 1.06 (*iso*-propyl cinnamate).

Polymerizations of methyl cinnamate derivatives (methyl 4-methyl cinnamate, methyl 4-methoxy cinnamate, methyl 3,4-dimethoxy cinnamate, and methyl 3,4,5-trimethoxy cinnamate) were performed to investigate the effect of substituents in the aromatic ring on the polymerization activity and properties of the obtained polymer. The molecular weight of the obtained polymer was slightly higher with methyl 4-methyl cinnamate (M_n = 8,300 g mol^{-1}) than with methyl cinnamate (M_n = 7,300 g mol^{-1}), although the polymer yields were similar (35%) (Entries 16 and 19, Table 1). In the case of methyl 4-methoxy cinnamate, the molecular weight of the obtained polymer was lower (M_n = 3,000 g mol^{-1}) but the polymer yield was higher than with methyl cinnamate (66% and 35%, respectively) (Entries 16 and 20, Table 1). Unfortunately, polymerization did not proceed when methyl 3,4-dimethoxy cinnamate and methyl 3,4,5-trimethoxy cinnamate were used as monomers.

Structural analysis of poly(methyl cinnamate). ^{1}H and ^{13}C NMR analyses of poly(methyl cinnamate) were performed to determine the molecular structure of the polymer. Figure 1 shows the ^{1}H and ^{13}C NMR spectra of the obtained poly(methyl cinnamate) (Entry 5, Table 1) and the methyl cinnamate monomer. The α-alkene proton peak (H_f, δ = 6.43 ppm) and the β-alkene proton peak (H_e, δ = 7.69 ppm) of the monomer (Fig. 1a) disappeared in the ^{1}H NMR spectrum of the obtained polymer (Fig. 1b). Further, signals (C_E, C_F) derived from the newly formed methylene skeleton were observed in the range of 40–60 ppm in the ^{13}C NMR spectrum of the obtained polymer[38] (Fig. 1d). These observations suggested that the carbon–carbon double bond moiety of the monomer was enchained and propagation proceeded.

Additionally, in the ^{1}H NMR spectrum of the obtained polymer, resonance peaks were observed for the methyl protons (H_L, H_M) at the initiation chain-end derived from MTS near 0.5 and 1.0 ppm; the methoxy protons (H_H, H_I) in the side chains and at the initiation chain-end, the methine protons (H_E, H_F) in the main chain, and the methylene proton (H_N) at the termination chain-end in the region of 1.7–4.0 ppm; and the phenyl protons (H_A, H_B, H_C) in the side chains in the region of 5.5–7.5 ppm[19,23]. However, all the peaks were broad.

The molecular structure of the polymer was also determined by MALDI-TOF-MS analysis of the obtained poly(methyl cinnamate) (Entry 12, Table 1). As shown in Fig. 2a, the mass spectrum

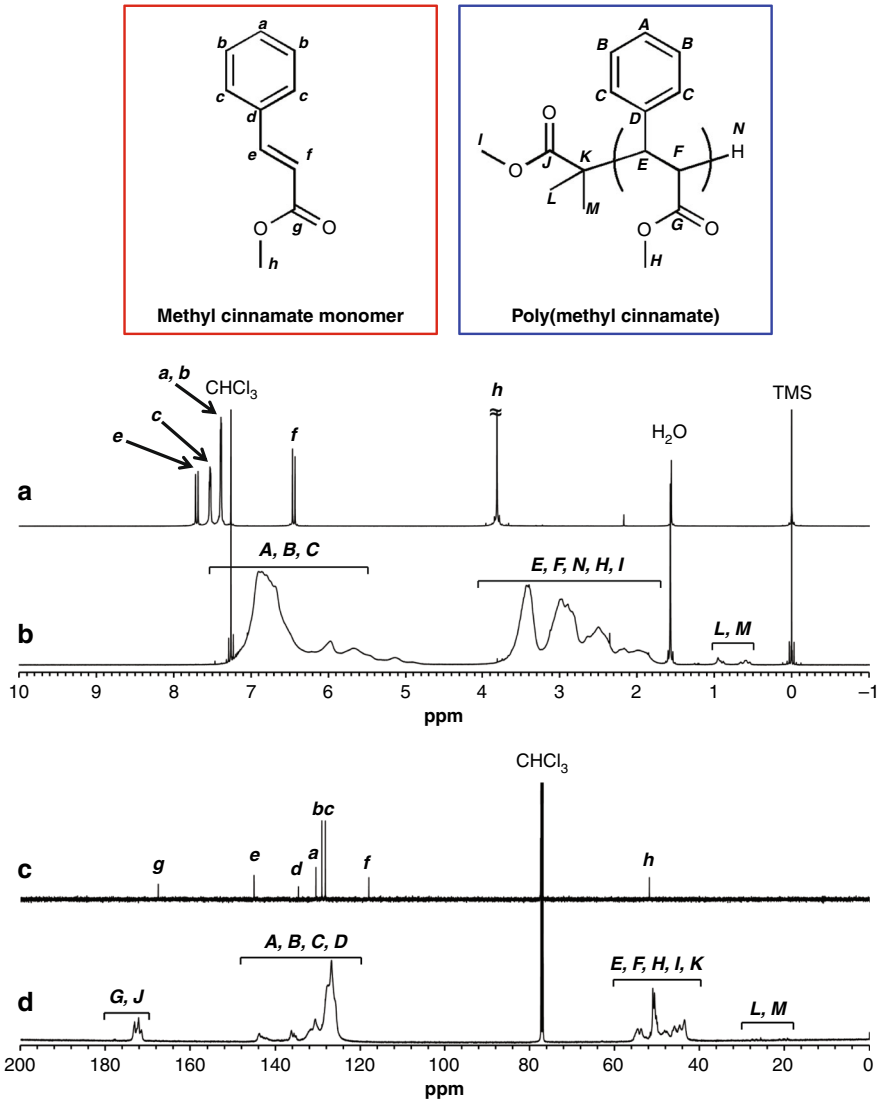

Fig. 1 ^{1}H and ^{13}C NMR spectra of methyl cinnamate monomer and poly(methyl cinnamate). **a** ^{1}H NMR spectrum of methyl cinnamate monomer. **b** ^{1}H NMR spectrum of poly(methyl cinnamate) (Entry 5, Table 1). **c** ^{13}C NMR spectrum of methyl cinnamate monomer. **d** ^{13}C NMR spectrum of poly(methyl cinnamate) (Entry 5, Table 1). ^{1}H NMR spectra were measured in $CDCl_3$ at room temperature and 500 MHz. ^{13}C NMR spectra were measured in $CDCl_3$ at room temperature and 125 MHz

mainly consists of one major series (**A**) and one minor series (**B**) of mass ions. For major series **A**, a plot of the m/z values against the repeat unit number (n) of methyl cinnamate monomers gave a straight line with a slope of $m/z = 162$ and an intercept of $m/z = 125$ (Fig. 2b). This slope corresponds to the mass of the methyl cinnamate monomer, and the intercept corresponds to the sum of the masses for a polymer chain-end with a formula of $C_5H_{10}O_2$ and Na^+ (derived from CF_3COONa added as an ionizing agent in the MALDI-TOF-MS measurement). This result clearly shows that the polymer of main series **A** has the structural formula $(CH_3)_2[CH_3OC(=O)]C$–(methyl cinnamate)$_n$–H. Herein, $(CH_3)_2[CH_3OC(=O)]C$ at the initiation chain-end is derived from MTS, whereas the methylene group at the termination chain-end is generated by acid treatment of the terminal silyl ether group in the living polymer (Supplementary Fig. 1).

By contrast, the polymer corresponding to minor series **B** is not considered to have the same molecular structure, even though series **B** also has mass ion intervals corresponding to a repeat unit of $m/z = 162$. A detailed analysis of the mass spectrum revealed that the polymer of minor series **B** corresponded to the loss of one methanol molecule from the polymer of main series **A**. Thus, the polymer of minor series **B** is considered to correspond to poly (methyl cinnamate) with a terminal cyclic structure, generated via the cyclization of the living chain-end (Supplementary Fig. 2). These results revealed that the polymers synthesized using the GTP system consist of mainly linear forms but may include terminal cyclic structures. Additionally, the presence of cyclic structures could be confirmed by the ketone carbons observed in the ^{13}C NMR analysis of the oligomer sample synthesized by the GTP of methyl cinnamate with MTS and Tf_2NTMS in CH_2Cl_2 at room temperature, as the cyclization reaction was promoted at this temperature (Supplementary Fig. 4).

Structural analysis of oligo(methyl cinnamate). We gained more detailed information about the structure of the obtained poly(methyl cinnamate) by analysing the structures of low-molecular-weight homologs.

Figure 3a–d shows the size-exclusion chromatography (SEC) curves for the synthesized mixture of low-molecular-weight

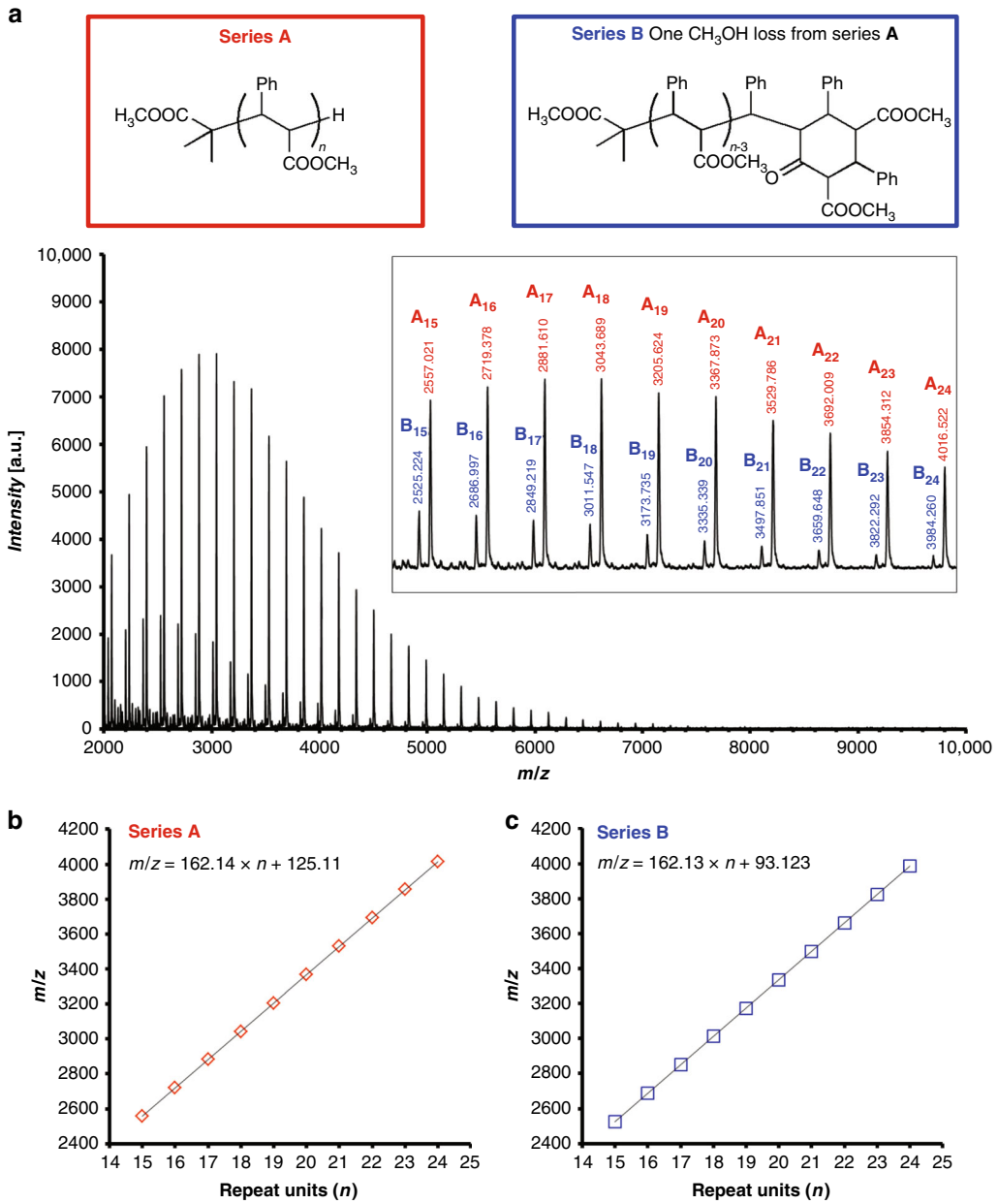

Fig. 2 MALDI-TOF-MS spectrum of poly(methyl cinnamate). **a** MALDI-TOF-MS spectrum of poly(methyl cinnamate) (Entry 12, Table 1). **b** Plot of *m/z* values of major series **A** vs the number of methyl cinnamate repeat units (*n*). **c** Plot of *m/z* values of minor series **B** vs the number of methyl cinnamate repeat units (*n*). MALDI-TOF-MS was measured using dithranol as a matrix and CF_3COONa as an ionizing agent

homologs and for the samples separated by SEC fractionation from the mixture. Each peak in Fig. 3a was characterized as a linear oligomer (trimer to hexamer) by ^{1}H NMR and MALDI-TOF-MS analyses (Supplementary Figs. 5–8). Figure 3e–g shows the ^{1}H NMR spectra of the separated oligomer samples (tetramer to hexamer). The proton resonance peaks of the oligomers substantially agreed with those of poly(methyl cinnamate) (Figs. 1b and 3e–g). When a linear oligomer has a polymerization degree of *N*, one molecule should contain $(N+1)$ methyl ester groups. By focusing on the region derived from the methyl ester groups, it could be inferred that each oligomer included multiple kinds of diastereomers because multiple sets of $(N+1)$ peaks were observed in each ^{1}H NMR spectrum (Fig. 3e–g). We separated the diastereomers by normal-phase high-performance liquid chromatography (HPLC) fractionation to acquire the isomers that are observed as a major component in the ^{1}H NMR spectrum.

Figure 4 shows the ORTEP representations of each isolated isomer. These molecular structures clearly show that each oligomer was composed of a linear saturated carbon–carbon skeleton with alternating phenyl groups and methyl ester groups in the side chains in a *head-to-tail* direction. Additionally, the relative conformations of the asymmetric carbon atoms in the main chains of the representative isomers exhibited $(et)_n ee$ sequences (*e*: *erythro*, *t*: *threo*) in the *head-to-tail* direction, corresponding to a disyndiotactic structure. The disyndiotactic selectivities of the oligomers, as calculated from the integral ratio of the proton resonance peaks derived from the terminal methyl groups in the ^{1}H NMR spectra, were 45% (tetramer), 30% (pentamer), and 22% (hexamer).

Thermal properties of poly(alkyl cinnamate) derivatives. We investigated the thermal properties (T_{d5}, T_{d50}, and T_g) of the

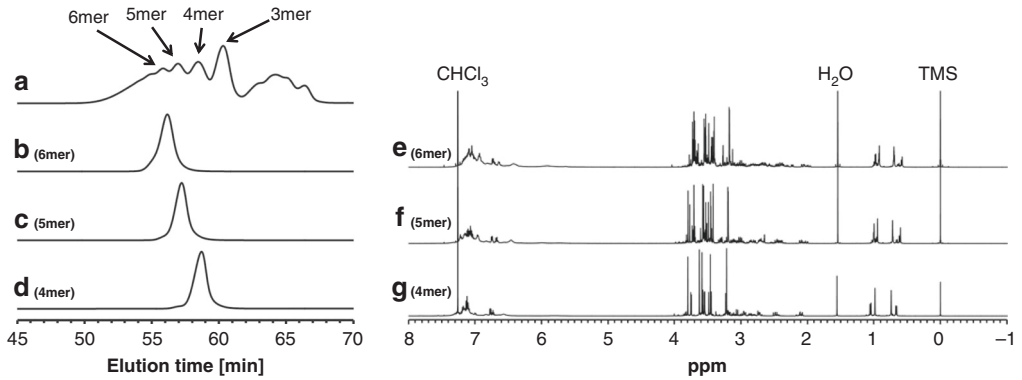

Fig. 3 Fractionation of low-molecular-weight homologs of poly(methyl cinnamate). **a** SEC curve of the mixture of low-molecular-weight homologs of poly (methyl cinnamate) synthesized by GTP in the presence of MTS and Tf_2NTMS. **b** SEC curve of the hexamer separated from the mixture. **c** SEC curve of the pentamer separated from the mixture. **d** SEC curve of the tetramer separated from the mixture. **e** ^1H NMR spectrum of the hexamer separated from the mixture. **f** ^1H NMR spectrum of the pentamer separated from the mixture. **g** ^1H NMR spectrum of the tetramer separated from the mixture

obtained polymers by TGA and DMA, as summarized in Table 2. Two representative poly(methyl cinnamate) samples (Entry 5, Table 1, $M_n = 15{,}000\ g\ mol^{-1}$; Entry 13, Table 1, $M_n = 4{,}600\ g\ mol^{-1}$) were evaluated. Despite the difference in molecular weight, the T_{d5} (340 °C and 341 °C) and T_{d50} values (377 °C and 374 °C) of these polymers were similar. Thus, within this molecular weight range, the molecular weight did not influence the T_d of poly(methyl cinnamate). In the case of poly(ethyl cinnamate) (Entry 17, Table 1), which has a bulkier ester substituent than poly(methyl cinnamate), the T_{d5} and T_{d50} values were lower than those of poly(methyl cinnamate). By contrast, the T_{d5} and T_{d50} values of poly(methyl 4-methoxy cinnamate) (Entry 20, Table 1) were the highest among the obtained polymers (358 °C and 407 °C, respectively).

For the two examined poly(methyl cinnamate) samples, the T_g values were similar (165 °C and 163 °C, respectively). In the case of poly(ethyl cinnamate), the T_g value was lower than that of poly (methyl cinnamate) (122 °C), as observed for the T_d results. The T_g value of poly(methyl 4-methyl cinnamate) (Entry 19, Table 1) was the highest among the obtained polymers (194 °C) (Supplementary Fig. 9). Previously, it has been reported that the T_g of *atactic*-poly (methyl methacrylate) (PMMA) is ~105–122 °C, the T_g of *syndiotactic*-PMMA is ~105–120 °C, the T_g of *isotactic*-PMMA is ~51–107 °C, and the T_g of PSt is ~85–107 °C[39]. Thus, the poly(alkyl cinnamate)s and derivatives synthesized using the GTP system have very high thermal stabilities, which are comparable to and even exceed that of polycarbonate ($T_g = 137$–154 °C), a well-known engineering plastic[39].

Discussion

Cinnamic monomers, which are known to be difficult to polymerize by classical polymerization methods, were successfully homopolymerized by the GTP technique through the general GTP mechanism. Compared with literature examples[10–18], our approach realized convenient homopolymerization of cinnamates under relatively mild conditions. This behavior is likely due to the easy repetition of the Michael reaction in the GTP system. The low temperature used for this reaction could suppress side reactions, allowing propagation to proceed preferentially. Notably, the bulkiness of the ester substituent was found to be an effective method of controlling the structure of the polymer main chain. For instance, the bulky ester of *iso*-propyl cinnamate suppressed the termination reactions, as confirmed by the low amount of terminal cyclic structures observed in the MALDI-TOF-MS analysis of poly(*iso*-propyl cinnamate) (Entry 18, Table 1) (Supplementary Fig. 10). Furthermore, the polymerization results for various methyl cinnamate derivatives (Entries 19–22, Table 1) suggested that the polymerization activity of the monomer is influenced considerably by the steric hindrance and/or the electronic contribution of the substituents on the aromatic ring.

Using this GTP technique, polymers with a linear saturated carbon–carbon skeleton and alternating side chains of aromatic rings and ester groups were generated, as confirmed by NMR and MALDI-TOF-MS analyses. Importantly, polymerization in this system proceeded only at the carbon–carbon double bond moiety of the monomer without the involvement of the conjugated aromatic ring, as indicated by NMR and X-ray crystallography analyses of the low-molecular-weight homologs (Supplementary Fig. 11). However, the stereoregularity of the obtained polymer was likely not very high, as broad peaks were observed in the ^1H NMR spectrum (Fig. 1b) and some terminal cyclic structures were detected by MALDI-TOF-MS analysis. By contrast, the low-molecular-weight homologs revealed some preference for disyndiotactic stereoregularity (Fig. 4). Thus, it is suggested that a *threo* addition and *trance* opening mechanism proceeded with some priority in our cinnamate polymerization system, as Ute and co-workers previously reported that the alkyl crotonate polymerization system forms a disyndiotactic polymer chain by a *threo* addition and *trance* opening mechanism[23,24] (Supplementary Fig. 12). However, in the case of the current GTP system, as the propagation reaction proceeds, the stereoregularity of the polymer decreases.

Surprisingly, the obtained polymers exhibited high thermal stabilities comparable to and even exceeding those of engineering plastics. The structural analyses clearly revealed that the poly(alkyl cinnamate)s and derivatives synthesized using the GTP system have substituents at both the α-position and the β-position in the main chain, which is expected to decrease the flexibility of the main chain. The increase in stiffness derived from the decrease in flexibility might have a considerable effect on the high thermal stability. Moreover, polymer stereoregularity, which is somewhat low at present, would affect the thermal stability to some extent, as a strong correlation between the tacticity and the thermal stability of PMMA is already known[40,41]. In the future, it is expected that high-performance polymer materials, such as super engineering plastics, can be produced by controlling the stereoregularity of the polymer. Therefore, we will study the efficiency of various monomers, initiators, and catalysts for the GTP system toward achieving the synthesis of highly stereoregular polymers.

Methods

Materials. Methyl cinnamate, ethyl cinnamate, and *iso*-propyl cinnamate were obtained from Tokyo Chemical Industry Co. (TCI) and were used without further purification. Methyl 4-methyl cinnamate, methyl 4-methoxy cinnamate, methyl 3,4-

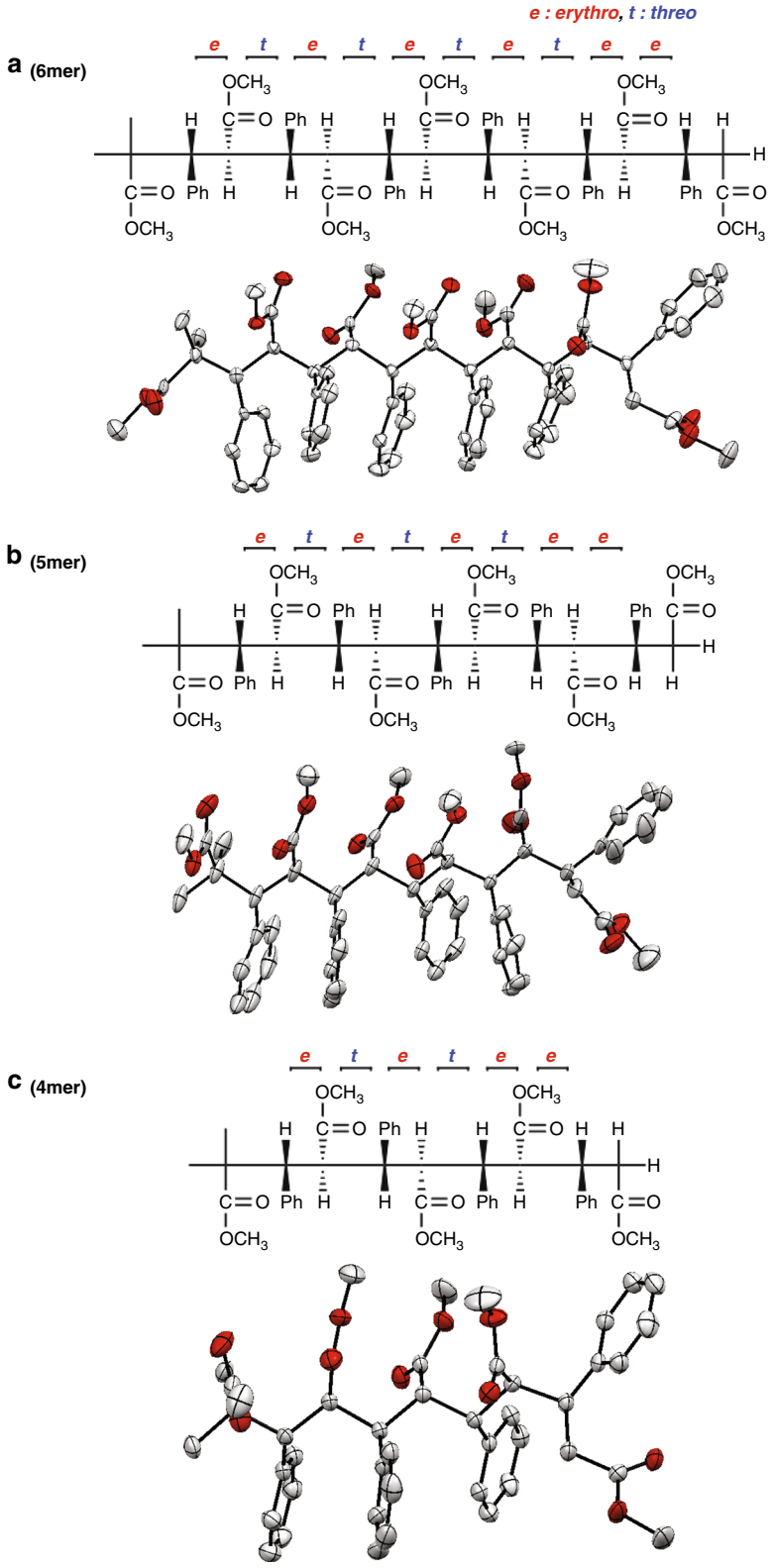

Fig. 4 ORTEP drawing of the X-ray crystal structure of disyndiotactic oligomers. **a** Hexamer of methyl cinnamate. **b** Pentamer of methyl cinnamate. **c** Tetramer of methyl cinnamate. All hydrogen atoms are omitted for clarity. Carbon atoms are shown in white and oxygen atoms are shown in red (thermal ellipsoids at the 50% probability level). The crystallographic data are summarized in Supplementary Table 1. Single crystals of methyl cinnamate oligomers suitable for X-ray crystallography were grown in a mixed solvent of $CHCl_3$/*n*-hexane

Table 2 Thermal properties (T_{d5}, T_{d50}, and T_g) of the polymers synthesized from various cinnamates and their derivatives

Polymer	M_n (g mol^{-1})	$Đ$ (M_w/M_n)	T_{d5}[a] (°C)	T_{d50}[a] (°C)	T_g[b] (°C)
Poly(methyl cinnamate)	15,000	1.69	340	377	165
Poly(methyl cinnamate)	4,600	1.30	341	374	163
Poly(ethyl cinnamate)	3,800	1.10	327	361	122
Poly(methyl 4-methyl cinnamate)	8,300	1.16	339	362	194
Poly(methyl 4-methoxy cinnamate)	3,000	1.48	358	407	145

[a] T_{d5} and T_{d50} are defined as the temperatures at which the weight loss reached 5% and 50%, respectively, of the total weight in a nitrogen atmosphere
[b] T_g is defined as the temperature corresponding to the maximum tan δ value in the DMA measurement

dimethoxy cinnamate, and methyl 3,4,5-trimethoxy cinnamate were prepared by esterification of the corresponding cinnamic acids (4-methylcinnamic acid, 4-methoxycinnamic acid, 3,4-dimethoxycinnamic acid, and 3,4,5-trimethoxycinnamic acid, which were obtained from TCI) with methanol in the presence of sulfuric acid according to the literature[42]. MTS (obtained from TCI) was distilled over CaH_2 and was stored at −35 °C in a glovebox. $C_6H_5CHTf_2$, Tf_2NH, Tf_2NTMS, $Ph_3C[B(C_6F_5)_4]$, and $CHCl_3$ were obtained from TCI and Wako Pure Chemical Industries and were used without further purification. Argon and nitrogen were used after purification by passing through a dry clean column (4A molecular sieves) and a Gas clean CC-XR column purchased from Nikka Seiko. CH_2Cl_2 (Kanto Chemical Co., super dehydrated grade) was purified via a SPS 800 system (MBraun).

Monomer synthesis. Methyl 4-methyl cinnamate was synthesized by the reaction of 4-methylcinnamic acid and methanol. 4-Methylcinnamic acid (24.9 g, 0.15 mol) and methanol (300 mL) were charged into a flask, followed by the dropwise addition of sulfuric acid (2.5 mL) with vigorous stirring at 60 °C. The mixture was refluxed for 5 h at 80 °C. After concentrating, the mixture was poured into saturated $NaHCO_3$ aq. and extracted with $CHCl_3$. Then, the organic layer was washed with water and brine, and dried over Na_2SO_4. After filtration, the organic layer was concentrated. The residue was dissolved in hexane, which was then evaporated until a white solid was separated. Cooling the solution yielded methyl 4-methyl cinnamate as white crystals (24.3 g, 89.6%). The syntheses of methyl 4-methoxy cinnamate (85.9% yield), methyl 3,4-dimethoxy cinnamate (78.8% yield), and methyl 3,4,5-trimethoxy cinnamate (93.6% yield) were carried out in a similar manner.

Polymerization. All manipulations were performed under a dry and oxygen-free argon atmosphere using standard high-vacuum Schlenk techniques or a glovebox. A typical polymerization procedure (Entry 10, Table 1) is as follows: methyl cinnamate (2.10 g, 13 mmol), MTS (45.1 mg, 0.26 mmol), and CH_2Cl_2 (5 mL) were charged into a Schlenk tube in a glovebox. A CH_2Cl_2 solution (2.5 mL) of Tf_2NTMS (91.5 mg, 0.26 mmol) was added to initiate the polymerization reaction at −35 °C. After a predetermined reaction period, methanol (10 mL) was poured into the reaction mixture, and then the solvents were removed by evaporation under reduced pressure. The residue was dissolved in $CHCl_3$, and the solution was poured into a large amount of hexane. The precipitated polymer was collected by filtration, washed several times with hexane, and dried under vacuum for 24 h. The polymerizations of various cinnamates and their derivatives using various organic acid catalysts were carried out in a similar manner.

Oligo(methyl cinnamate) synthesis for X-ray analysis. Methyl cinnamate (4.05 g, 25 mmol), MTS (1.45 g, 8.3 mmol), and CH_2Cl_2 (2.5 mL) were charged into a Schlenk tube in a glovebox. A CH_2Cl_2 solution (6.5 mL) of Tf_2NTMS (88.3 mg, 0.25 mmol) was added to initiate the reaction at −35 °C. After 5 h, the reaction was terminated by adding 10 mL of methanol. The mixture was evaporated under reduced pressure to remove the volatile components. Then, 40 mL of $CHCl_3$ was added to the residue. The $CHCl_3$-insoluble part was removed by filtration, and the sample of mixed oligomers was obtained as the $CHCl_3$-soluble part.

Fractionation of oligomers. Previously, Ute and co-workers reported the single-crystal X-ray structural analysis of alkyl crotonate oligomers separated by SEC and HPLC to determine the configuration of the disyndiotactic stereospecific poly(alkyl crotonate) synthesized by GTP using HgI_2 or CdI_2 as a catalyst and iodotrialkylsilane as a cocatalyst[23,24,43]. Therefore, we used a similar strategy to determine the structures of the obtained poly(alkyl cinnamate)s.

Fractionation by SEC was performed at room temperature using a preparative HPLC system (Shimadzu LC-20AR Semi-Preparative Solvent Delivery Unit, Shimadzu RID-10A Refractive Index Detector, and Shimadzu DGU-20A 3 R Degassing Unit) equipped with a Shodex K-2001 column (20.0 mm ID × 300 mm; pore size, 6 μm; plate number, >18,000; exclusion limit, 1500) and three Shodex K-802 columns (8.0 mm ID × 300 mm; pore size, 6 μm; plate number, >18,000; exclusion limit, 5000) using $CHCl_3$ as the mobile phase at a flow rate of 1.0 mL min^{-1}. The injection volume for each fractionation step was 300 μL. The weight yield of each oligomer was as follows: 15.2 wt% (larger than hexamer), 8.6 wt% (hexamer), 12.2 wt% (pentamer), 13.8 wt% (tetramer), 21.5 wt% (trimer), and 28.6 wt% (smaller than trimer).

Fractionation by normal-phase HPLC was performed at room temperature using the same system as for SEC fractionation, with the exception of the stationary and mobile phases. Two Develosil 100–5 columns (10.0 mm ID × 250 mm) were used as the stationary phase and a mixture of CH_3CN and *n*-butyl chloride (9:91, v/v) was used as the mobile phase at a flow rate of 2.0 mL min^{-1}. The injection volume for each fractionation step was 100 μL.

Measurements. All molecular weight data of polymer samples were obtained by SEC at 40 °C, using a Shimadzu GPC system equipped with an RID-10A refractive index detector, a Shodex GPC K-802 column, and a Shodex GPC K-806M column. $CHCl_3$ was used as the eluent at a flow rate of 0.8 mL min^{-1}, and a sample concentration of 1.0 mg mL^{-1} was applied. PSt standards with a low polydispersity were used to make a calibration curve.

^{1}H NMR and ^{13}C NMR measurements of the polymer and low-molecular-weight homolog samples were carried out on a Varian NMR system. The samples were dissolved in $CDCl_3$ and the 500 MHz ^{1}H NMR spectra were recorded at room temperature. The data was calibrated against tetramethylsilane (TMS, δ 0.00). The 125 MHz ^{13}C NMR spectra recorded at room temperature in a $CDCl_3$ solution. The data was calibrated against TMS (δ 0.00). The data were analyzed using the JEOL ALICE 2 and Mnova NMR software.

MALDI-TOF-MS analyses were conducted using an ultrafleXtreme MALDI-TOF spectrophotometer (Bruker Daltonics) operating in the linear or reflection mode at an accelerating voltage of 20 kV. The samples for MALDI-TOF-MS were prepared by mixing the obtained polymer or oligomer (30 mg mL^{-1}, 2 μL), the matrix (1,8-dihydroxy-9(10 *H*)-anthracenone (dithranol), 10 mg mL^{-1}, 2 μL), and the ionizing agent (sodium trifluoroacetate, 10 mg mL^{-1}, 8 μL) in THF, and then depositing the mixture on an MTP 384 target plate ground steel T F. External calibration was conducted prior to data acquisition. The detected mass list was extracted using the FlexAnalysis software (Bruker Daltonics).

X-ray diffraction data collection was performed on a Rigaku XtaLAB P200 diffractometer equipped with a DECTRIS PILATUS 200 K hybrid pixel array detector (HPAD), using a 3 kW sealed tube of Mo Kα radiation (λ = 0.71073 Å) at -100 °C. The Bravais lattice and the unit cell parameters were determined by the CrysAlisPro version 171.38.46 software package. The raw frame data were processed and absorption corrections were done using CrysAlisPro. The structure was solved using SIR-2014[44] and SHELXL-2018[45]. Structural refinement was performed using the WINGX-Version 2014.1 system[46], on F^2 anisotropically for all of the non-hydrogen atoms by the full-matrix least-squares method. The hydrogen atoms were placed at the calculated positions and were included in the structure calculation without further refinement of the parameters. The residual electron densities were of no chemical significance. The methyl ester groups (C(1), C(2), C(57), C(58), O(1), O(2), O(13), O(14)) of the pentamer were modeled as disordered at 50% occupancy. The methyl carbons (C(13), C(56)) of the pentamer were modeled as disordered over two positions at 70% and 30% occupancies, respectively.

CCDC numbers 1898516 (hexamer), 1898517 (pentamer), and 1898515 (tetramer) contain the supplementary crystallographic data for this paper. These data can be obtained free of charge from The Cambridge Crystallographic Data Centre via www.ccdc.cam.ac.uk/data_request/cif. The CIFs are also provided as Supplementary Data 1–3.

TGA was performed on a SII Nano Technology TG/DTA7200 thermal analyser from room temperature to 500 °C under a nitrogen atmosphere at a heating rate of 10 °C min^{-1}. T_{d5} is defined as the temperature at which the weight loss reaches 5% of the total weight. T_{d50} is defined as the temperature at which the weight loss reaches 50% of the total weight.

The T_g of each polymer was measured by DMA (Perkin Elmer DMA800) under a nitrogen atmosphere, by cooling the sample to −150 °C at 10 °C min^{-1}, and then recording the DMA scan from −150 to + 300 °C at a heating rate of 5 °C min^{-1} and a frequency of 1 Hz.

Data availability

Crystallographic data for the structures of the methyl cinnamate oligomers have been deposited in the Cambridge Crystallographic Data Centre under codes 1898516 (hexamer), 1898517 (pentamer), and 1898515 (tetramer). These data can be obtained free of charge from The Cambridge Crystallographic Data Centre via www.ccdc.cam.ac.uk/data_request/cif.

Received: 24 March 2019 Accepted: 23 August 2019
Published online: 16 September 2019

References

1. Kimura, Y. & Ohara, H. *New Development of Bio-based Materials*. (CMC Publishing, Tokyo, 2007).
2. Ebnesajjad, S. *Handbook of Biopolymers and Biodegradable Plastics*. (Elsevier, Oxford, 2013).
3. Li, Y., Luo, X. & Hu, S. *Bio-based Polyols and Polyurethanes* (Springer, Cham, 2015).
4. Lambert, S. & Wagner, M. Environmental performance of bio-based and biodegradable plastics: the road ahead. *Chem. Soc. Rev.* **46**, 6855–6871 (2017).
5. Tabata, Y. & Abe, H. Synthesis and properties of alternating copolymers of 3-hydroxybutyrate and lactate units with different stereocompositions. *Macromolecules* **47**, 7354–7361 (2014).
6. Suvannasara, P. et al. Biobased polyimides from 4-aminocinnamic acid photodimer. *Macromolecules* **47**, 1586–1593 (2014).
7. Guoruoluo, Y. et al. Chemical constituents from the immature buds of Cinnamomum cassia (Lauraceae). *Biochem. Syst. Ecol.* **78**, 102–105 (2018).
8. Belgacem, M. N. & Gandini, A. *Monomers, Polymers and Composites from Renewable Resources*. (Elsevier, Amsterdam, 2008).
9. Zakzeski, J., Bruijnincx, P. C. A., Jongerius, A. L. & Weckhuysen, B. M. The catalytic valorization of lignin for the production of renewable chemicals. *Chem. Rev.* **110**, 3552–3599 (2010).
10. Sapiro, R. H., Linstead, R. P. & Newitt, D. M. Liquid-phase reactions at high pressures. Part II. The polymerisation of olefins. *J. Chem. Soc.* 1784–1790 (1937).
11. Marvel, C. S. & McCain, G. H. Polymerization of esters of cinnamic acid. *J. Am. Chem. Soc.* **75**, 3272–3273 (1953).
12. Matsumoto, A., Horie, A. & Otsu, T. Synthesis of substituted polymethylenes from alkyl cinnamates bearing bulky alkyl ester groups. *Eur. Polym. J.* **28**, 213–217 (1992).
13. Holmes-Walker, W. A. & Weale, K. E. Liquid-phase reactions at high pressure. Part IX. The polymerisation of some 1:2-disubstituted ethylenes. *J. Chem. Soc.* 2295–2301 (1955).
14. Hemmings, R. L. & Weale, K. E. Rates of polymerization of diethyl fumarate and trans-ethyl cinnamate at high pressures. *Polymer* **27**, 1819–1822 (1986).
15. Weale, K. E. Hindered initiation, primary-radical termination and effects of pressure on polymerization rates. *Polymer* **28**, 2151–2156 (1987).
16. Natta, G., Peraldo, M. & Farina, M. US Patent 3 259, 612 (1966).
17. Tsuruta, T., Makimoto, T. & Tanabe, K. Anionic polymerization of β-substituted acrylic esters. *Makromol. Chem.* **114**, 182–200 (1968).
18. Graham, R. K., Moore, J. E. & Powell, J. A. Preparation and properties of polymers of secondary alkyl crotonates and related monomers. *J. Appl. Polym. Sci.* **11**, 1797–1805 (1967).
19. Terao, Y., Satoh, K. & Kamigaito, M. Controlled radical copolymerization of cinnamic derivatives as renewable vinyl monomers with both acrylic and styrenic substituents: Reactivity, regioselectivity, properties, and functions. *Biomacromolecules* **20**, 192–203 (2019).
20. Miller, M. L. & Skogman, J. Polymerization of tert-butyl crotonate. *J. Polym. Sci. Part A* **2**, 4551–4558 (1964).
21. Makimoto, T., Tanabe, K. & Tsuruta, T. Anionic polymerization of methyl crotonate. *Makromol. Chem* **99**, 279–281 (1966).
22. Tsuruta, T., Makimoto, T. & Miyazako, T. Reaction modes and polymerization of crotonic esters with lithium aluminum hydride. *Makromol. Chem.* **103**, 128–139 (1967).
23. Ute, K. et al. Preparation of disyndiotacticpoly(methyl crotonate) by stereospecific group transfer polymerization. *Polym. J.* **31**, 177–183 (1999).
24. Ute, K., Asada, T. & Hatada, K. Highly "diheterotactic" polymerization of tert-butyl crotonate. *Macromolecules* **29**, 1904–1909 (1996).
25. Webster, O. W., Hertler, W. R., Sogah, D. Y., Farnham, W. B. & RajanBabu, T. V. Group-transfer polymerization. 1. A new concept for addition polymerization with organosilicon initiators. *J. Am. Chem. Soc.* **105**, 5706–5708 (1983).
26. Hertler, W. R., Sogah, D. Y., Webster, O. W. & Trost, B. M. Group-transfer polymerization. 3. Lewis acid catalysis. *Macromolecules* **17**, 1415–1417 (1984).
27. Sogah, D. Y., Hertler, W. R., Webster, O. W. & Cohen, G. M. Group transfer polymerization. Polymerization of acrylic monomers. *Macromolecules* **20**, 1473–1488 (1987).
28. McGraw, M. & Chen, E. Y.-X. Catalytic Lewis pair polymerization of renewable methyl crotonate to high-molecular-weight polymers. *ACS Catal.* **8**, 9877–9887 (2018).
29. McGraw, M. L. & Chen, E. Y.-X. Borane/silane frustrated Lewis pairs for polymerization of β-substituted Michael acceptors. *Tetrahedron* **75**, 1475–1480 (2019).
30. Zhang, Y. & Chen, E. Y.-X. Controlled polymerization of methacrylates to high molecular weight polymers using oxidatively activated group transfer polymerization initiators. *Macromolecules* **41**, 36–42 (2008).
31. Kakuchi, R. et al. Strong Brønsted acid as a highly efficient promoter for group transfer polymerization of methyl methacrylate. *Macromolecules* **42**, 8747–8750 (2009).
32. Hong, M., Chen, J. & Chen, E. Y.-X. Polymerization of polar monomers mediated by main-group Lewis acid–base pairs. *Chem. Rev.* **118**, 10551–10616 (2018).
33. Takenaka, Y. & Abe, H. Group-transfer polymerization of various crotonates using organic acid catalysts. *Macromolecules* **52**, 4052–4058 (2019).
34. Takenaka, Y. & Abe, H. JP Patent 6 342, 699 (2018).
35. Brittain, W. J. & Dicker, I. B. Isomerization of silyl ketene acetals: models for the propagating chain end in group transfer polymerization. *Polym. Int.* **30**, 101–107 (1993).
36. Brittain, W. J. & Dicker, I. B. Termination processes in group transfer polymerization. *Makromol. Chem. Macromol. Symp.* **67**, 373–386 (1993).
37. Brittain, W. J. & Dicker, I. B. Termination in group transfer polymerization. *Macromolecules* **22**, 1054–1057 (1989).
38. Neppel, A. & Butler, I. S. ^{13}C NMR spectra of poly(methyl methacrylate) and poly(ethyl methacrylate). *J. Mol. Struct.* **117**, 109–115 (1984).
39. Wypych, G. *Handbook of Polymers*. (ChemTec Publishing, Toronto, 2012).
40. Denny, L. R., Boyer, R. F. & Ellas, H.-G. Dependence of Tg and T_{II} on tacticity of PMMA by differential scanning calorimetry. *J. Macromol. Sci. Part B: Phys.* **25**, 227–265 (1986).
41. Chang, L. & Woo, E. M. Tacticity effects on glass transition and phase behavior in binary blends of poly(methyl methacrylate)s of three different configurations. *Polym. Chem.* **1**, 198–202 (2010).
42. Peterson, J. R., Russell, M. E. & Surjasasmita, I. B. Synthesis and experimental ionization energies of certain (E)-3-arylpropenoic acids and their methyl esters. *J. Chem. Eng. Data* **33**, 534–537 (1988).
43. Ute, K., Tarao, T. & Hatada, K. Group transfer polymerization of methyl crotonate. *Polym. J.* **29**, 957–958 (1997).
44. Burla, M. C., et al. SIR-2014, version 14.07. Institute of Crystallography, CNR: Italy, 2014.
45. Sheldrick, G. M SHELXL 2018/1. University of Göttingen: Germany, 2018.
46. Farrugia, L. J. WinGX and ORTEP for Windows: an update. *J. Appl. Crystallogr.* **45**, 849–854 (2012).

Acknowledgements

We thank Masayoshi Nishiura from the organometallic research team at RIKEN for collection and analysis of the X-ray crystal data. This research was financially supported by JSPS KAKENHI Grant Numbers 26410199 and 18K05210.

Author contributions

Y.T. conceived, designed, and directed the project. M.I., Y.T. and H.H. performed the experiments and analyzed the data. M.I. and Y.T. co-wrote the paper. M.I., Y.T., H.H., T.H. and H.A. discussed the results and commented on the manuscript.

Additional information

Supplementary information accompanies this paper at https://doi.org/10.1038/s42004-019-0215-3.

Competing interests: The authors declare no competing interests.

Reprints and permission information is available online at http://npg.nature.com/reprintsandpermissions/

Publisher's note Springer Nature remains neutral with regard to jurisdictional claims in published maps and institutional affiliations.